

LLM-Adapted Interpretation Framework for Machine Learning Models

Yuqi Jin¹, Zihan Hu¹, Weiteng Zhang², Weihao Xie¹, Jianwei Shuai^{3,4},
Xian Shen^{2,}, Zhen Feng^{1,3,4,*}*

1 College of Information and Engineering, First Affiliated Hospital,

Wenzhou Medical University, Wenzhou, China

2 Department of Gastrointestinal Surgery, First Affiliated Hospital,

Wenzhou Medical University, Wenzhou, China

3 Wenzhou Institute, University of Chinese Academy of Sciences, Wenzhou, China

4 Oujiang Laboratory (Zhejiang Lab for Regenerative Medicine, Vision and Brain Health), Wenzhou, China

*Correspondence:

shenxian@wmu.edu.cn (X.S.); zfeng2019@foxmail.com (Z.F.)

Abstract—Background & Aims: High-performance machine learning models like XGBoost are often "black boxes," limiting their clinical adoption due to a lack of interpretability. This study aims to bridge the gap between predictive accuracy and narrative transparency for sarcopenia risk assessment.

Methods: We propose the LLM-Adapted Interpretation Framework (LAI-ML), a novel knowledge distillation architecture. LAI-ML transforms feature attributions from a trained XGBoost model into a probabilistic format using specialized techniques (HAGA and CACS). A Large Language Model (LLM), guided by a reinforcement learning loop and case-based retrieval, then generates data-faithful diagnostic narratives.

Results: The LAI-ML framework achieved 83% prediction accuracy, significantly outperforming the baseline XGBoost model, 13% higher. Notably, the LLM not only replicated the teacher model's logic but also corrected its predictions in 21.7% of discordant cases, demonstrating enhanced reasoning.

Conclusion: LAI-ML effectively translates opaque model predictions into trustworthy and interpretable clinical insights, offering a deployable solution to the "black-box" problem in medical AI.

Keywords—Explainable AI (XAI), Knowledge Distillation, Large Language Models (LLM), Sarcopenia, XGBoost, SHAP (SHapley Additive exPlanations), Clinical Decision Support, Interpretability, Reinforcement Learning

INTRODUCTION

Sarcopenia, a progressive and debilitating loss of skeletal muscle mass and function, is an escalating public health concern in aging populations, projected to affect over 200 million individuals by 2050. Despite advancements in diagnostic tools, existing paradigms—such as dual-energy X-ray absorptiometry and consensus-based criteria—suffer from high variability and limited sensitivity to early-stage disease, resulting in delayed interventions and increased morbidity [1].

Machine learning (ML) models, particularly gradient-boosted frameworks like XGBoost, have demonstrated remarkable performance in predictive tasks [2]. However, their "black-box" nature severely limits clinical adoption, as

physicians struggle to interpret complex decision boundaries and abstract feature attributions like those produced by SHapley Additive exPlanations (SHAP) [3].

Large language models (LLMs), by contrast, can generate fluent, human-readable narratives, but when detached from underlying statistical evidence, they are prone to hallucinations, that is, generating plausible yet unfaithful explanations [4,5]. This epistemic dissonance between numerical rigor and narrative coherence creates a methodological gap[6,7]: current workflows treat prediction and explanation as separate tasks, leaving clinicians with tools that are either too opaque or too unreliable.

To address this, we propose the LLM-Adapted Interpretation Framework for Machine Learning Models (LAI-ML), a hybrid architecture that integrates SHAP-based feature attribution [8] with language model generation through a novel transformation pipeline. By distilling SHAP outputs into probabilistic formats via Half-Step Aligned Group Averaging (HAGA) and Contrastive Attribution via Sigmoid (CACS), LAI-ML enables an LLM to generate concise, data-faithful diagnostic narratives aligned with the logic of the predictive model. A lightweight reinforcement-style calibration loop further optimizes agreement between the LLM and XGBoost outputs, reducing hallucination while preserving linguistic fluency[9,10]. In validation across over 9,000 clinical cases, LAI-ML maintains predictive fidelity while significantly improving interpretability, offering a clinically deployable path forward for transparent, AI-assisted decision-making in geriatric care.

METHODS

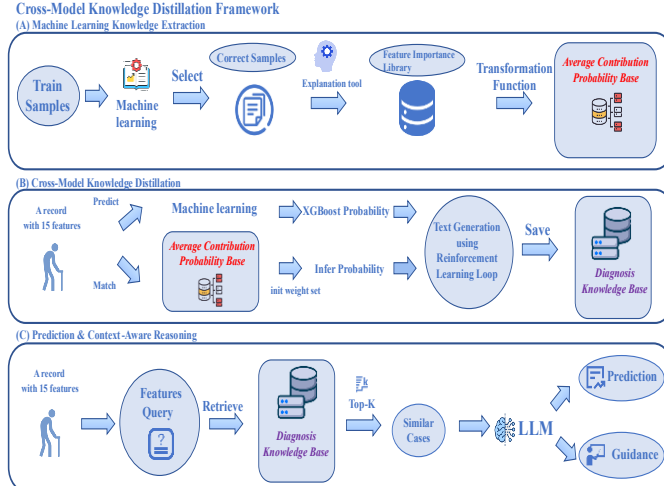


Figure 1. The architecture of the Cross-Model Knowledge Distillation(CMKD)framework. The framework is composed of three core modules: (A) Machine Learning Knowledge Extraction, which trains an XGBoost model and distills its feature knowledge into an Average Contribution Probability Base (ACPB); (B) Cross-Model Knowledge Distillation, which uses a reinforcement-learning loop to align Large Language Model's (LLM) outputs with the XGBoost model's predictions, generating a Diagnosis Knowledge Base (DKB); and (C) Prediction & Context-Aware Reasoning, where for a new case, similar precedents are retrieved from the DKB to help the LLM generate a final prediction and actionable guidance.

Figure 1 shows the three stages of the framework:

Module (A) Machine Learning Knowledge Extraction

We begin by training an XGBoost model on the original dataset and selecting only those samples it predicts correctly. Using an explainability tool (e.g., SHAP) [3], we build a “Feature Importance Library,” then transform per-feature importance into contribution probabilities to form an Average Contribution Probability Base (ACPB).

Module (B) Cross-Model Knowledge Distillation

In this module, at first, we compare the XGBoost output probabilities with inferred probabilities calculated by contribution probabilities from the ACPB and initial weight set. We then prompt a large language model (LLM) to activate reinforcement-learning loop to generate diagnosis texts [11,12] and save them into Diagnosis Knowledge Base.

Module (C) Prediction & Context-Aware Reasoning

For a new input, we retrieve the Top-K most similar cases from the Diagnosis [13] Knowledge Base (DKB) by feature values. We feed these similar cases, together with the feature values, into the LLM. The LLM then issues both a class prediction and actionable guidance grounded in those precedents.

In summary, **Cross-Model Knowledge Distillation** (CMKD) seamlessly fuses XGBoost’s numerical predictive power with an LLM’s semantic reasoning ability—preserving high accuracy while greatly enhancing interpretability and practical utility. Detailed algorithmic designs, hyperparameter settings, and experimental evaluations are deferred to the following sections.

2.1 Data processing

We utilize (Here, I plan to include the CHARLS[14] data, with the specific processing methods detailed in the appendix.).

To achieve model balance, we select 300 records from normal individuals and combine them with all 300 records of sarcopenia patients. Additionally, to guarantee the effectiveness of the model and training efficiency, we choose 15 features based on feature importance. These features consist of 11 physical characteristics and 4 mental characteristics.

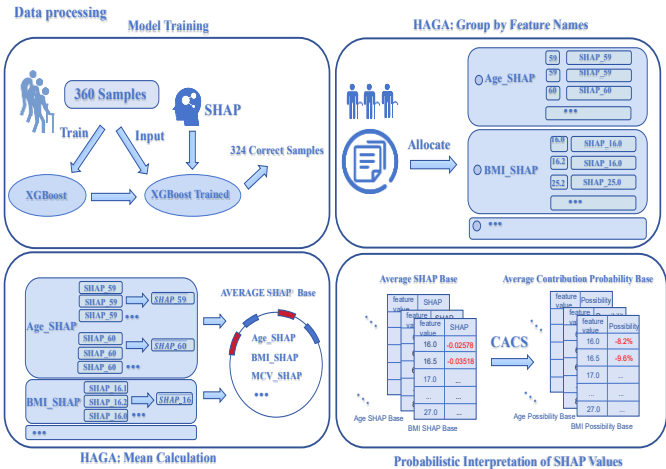


Figure 2. Detailed workflow of the knowledge transformation pipeline.

This figure illustrates the four key steps in converting raw sample data into a probabilistic knowledge base for the LLM. It begins with (1) Data processing and Model Training using XGBoost and SHAP. This is followed by (2) HAGA: Group by Feature Names, where SHAP values are allocated to their respective features. Then, (3) HAGA: Mean Calculation computes the average SHAP value for discretized feature intervals. Finally, (4) Probabilistic

Interpretation of SHAP Values uses the Contrastive Attribution via Sigmoid (CACS) method to transform these averaged SHAP values into contribution probabilities.

2.2. Module (A) Machine Learning Knowledge Extraction

2.2.1 XGBboost training and SHAP Explanation

In our methodology, we employ XGBoost-Regressor as the teacher model in our knowledge distillation framework, shown in Figure 2, Model Training, leveraging its demonstrated stability and predictive accuracy for sarcopenia probability estimation and use SHAP module to explain the prediction mechanism [15]. The dataset undergoes stratified partitioning into three distinct subsets: a training set containing 360 samples (60% of total data), a validation set with 180 samples (30%), and a test set comprising 60 samples (10%). Through hyperparameter optimization with [190] boosting rounds and a maximum tree depth of [8], we developed a sarcopenia prediction model that achieves 90% training accuracy while maintaining 73% validation accuracy and 70% test accuracy. Then, we use SHapley Additive exPlanations (SHAP) to explain features by calculating SHAP values of every feature.

2.2.2 Average Contribution Probability Base building

Following the development of our XGBoost-Regressor model and SHAP Explanation, we integrated them with a new approach to construct an interpretable knowledge base.

This systematic approach, consisting of Half-step Aligned Group Averaging and Probabilistic Interpretation of SHAP Values, enables quantification of feature contributions and latent pattern extraction, thereby constructing an actionable knowledge base for LLM to assessment through evidence-based sarcopenia.

2.2.3 Half-step Aligned Group Averaging

After former sections, we got a 324×15 Feature-SHAP Matrix:

$$\text{Feature - SHAP Matrix} = \begin{bmatrix} s_1 \\ s_2 \\ \vdots \\ s_{324} \end{bmatrix} = \begin{bmatrix} f_{1,1} & f_{1,2} & \dots & f_{1,15} \\ f_{2,1} & f_{2,2} & \dots & f_{2,15} \\ \vdots & \vdots & \ddots & \vdots \\ f_{324,1} & f_{324,2} & \dots & f_{324,15} \end{bmatrix}$$

where s_i is the i -th correct sample and $f_{i,j}$ is the j -th feature value with its SHAP value in the i -th correct sample.

And it is hard to directly utilize the SHAP values as a cross-model bridge due to the discrepancy between population-level statistics and individual feature distributions. To align SHAP values with both population-level statistics and individual feature distributions, we propose a three-stage discretization framework based on adaptive interval grouping, named Half-step Aligned Group Averaging[16], shown in Figure 2.

The core of this approach is to group feature values by feature names and compute mean SHAP values per group using predefined non-overlapping intervals with a fixed step size unit. The detailed workflow is outlined below:

Stage 1: HAGA Group by Feature Names and Intervals

Group by Feature Names:

Initially, for a given 324×15 Feature-SHAP Matrix, we carried out a transposition operation on it, thereby acquiring a Feature Set containing 15 sub-feature sets. Within each of these feature sets, there are 324 feature values accompanied by their respective corresponding SHAP values:

$$\text{Feature - SHAP Matrix}^T = \text{Feature Set} = \begin{bmatrix} F_1 \\ F_2 \\ \vdots \\ F_{15} \end{bmatrix} = \begin{bmatrix} f_{1,1} & f_{2,1} & \dots & f_{324,1} \\ f_{1,2} & f_{2,2} & \dots & f_{324,2} \\ \vdots & \vdots & \ddots & \vdots \\ f_{1,15} & f_{2,15} & \dots & f_{324,15} \end{bmatrix}$$

Where F_i is the i -th feature set and $f_{i,j}$ is the j -th feature value with its SHAP value in the i -th correct sample. Then, we can group feature and SHAP values in one certain feature set.

Interval Construction:

There two types of features, continuous features and integer features.

For continuous and integer features in the dataset, this study proposes a unified interval partitioning rule to achieve discretization and structured representation of feature values. For **continuous features**, an equidistant midpoint partitioning approach is adopted: a midpoint sequence $X = \{x_m | x_m = 0.5m, m \in \mathbb{Z}\}$ is generated with a step size of 0.5. Each midpoint defines a closed interval of width 0.5, specifically $[x_m - 0.25, x_m + 0.25]$, which encompasses all continuous values within ± 0.25 of x_m . For example, midpoint 0.5 corresponds to the interval [0.25, 0.75], midpoint 1.0 corresponds to [0.75, 1.25], and so on.

For **integer features**, the interval partitioning simplifies to an exact matching rule: the feature value must strictly equal the specified midpoint x_m (where $x_m \in \mathbb{Z}$). That is, only when the feature value $V = x_m$ is the sample assigned to the interval group centered at x_m . This rule ensures that the discretization results of integer features have clear boundaries and uniqueness. To establish a bijective correspondence between feature values and discrete intervals, the following formal grouping rule is defined: For any feature value V , if it satisfies one of the following conditions, it is assigned to the corresponding interval group g :

Continuous feature value: There exists a midpoint x_m such that $x_m - 0.25 \leq V \leq x_m + 0.25$;

Integer feature value: $V = x_m$ (where x_m is an integer midpoint).

This mapping rule ensures that each feature value uniquely belongs to one interval group, and each interval group contains all feature values and their corresponding SHAP values that meet the condition. Through this operation, the original feature space is transformed into a set of finite discrete intervals, providing structured input for subsequent knowledge distillation.

After interval partitioning and grouping mapping, Feature Set is organized into the following matrix form:

$$\text{Assigned Feature Set} = \begin{bmatrix} F_1 \\ F_2 \\ \vdots \\ F_{15} \end{bmatrix} = \begin{bmatrix} g_{1,1} & g_{1,2} & \dots & g_{1,k_1} \\ g_{2,1} & g_{2,2} & \dots & g_{2,k_2} \\ \vdots & \vdots & \ddots & \vdots \\ g_{15,1} & g_{15,2} & \dots & g_{15,k_{15}} \end{bmatrix}$$

Where F_i is the i -th feature interval group set, g is the interval group in one certain interval and k_i is the length of interval in the i -th feature interval group set.

Subsequently, based on the discretized feature intervals, we obtained the corresponding sets of SHAP and feature values for each interval. These sets reflect the degree of influence that feature values within specific ranges have on sarcopenia prediction, providing preliminary insights into local feature effects.

However, when attempting to estimate the SHAP value of a new feature value by referencing similar feature values within existing interval groups, we still encounter the challenge of

ambiguous multi-feature-values matching in one certain interval group — where the new feature value could be plausibly closed to many feature values.

Stage 2: HAGA Mean Calculation:

We calculate the arithmetic mean of all values V within the same interval to serve as the representative value for that group to solve the ambiguous multi-feature-values matching challenge.

By establishing clear - cut interval boundaries and discretization rules, this method effectively eliminates the ambiguity associated with traditional rounding techniques. Simultaneously, it ensures computational efficiency and maintain interpretability. It finds wide applications in data standardization, noise filtering, and feature engineering tasks. For all SHAP values within the i -th interval compute the mean:

$$\bar{s}_i = \frac{1}{N} \sum_{v \in \text{group}_i} V$$

where N is the count number of SHAP values in the i -th group. Through former two stages, we systematically processed the SHAP values to enhance useability of SHAP knowledge. The methodology yields 15 specialized feature SHAP knowledge sub-bases:

$$\text{SHAP Knowledge Base} = \begin{bmatrix} b_1 \\ b_2 \\ \vdots \\ b_{15} \end{bmatrix} = \begin{bmatrix} \bar{s}_{1,1} & \bar{s}_{1,2} & \cdots & \bar{s}_{1,k_1} \\ \bar{s}_{2,1} & \bar{s}_{2,2} & \cdots & \bar{s}_{2,k_2} \\ \vdots & \vdots & \ddots & \vdots \\ \bar{s}_{15,1} & \bar{s}_{15,2} & \cdots & \bar{s}_{15,k_{15}} \end{bmatrix}$$

Where b_i is the i -th feature SHAP knowledge sub-bases, \bar{s} is the mean SHAP value in one certain interval and k_i is the length of mean SHAP value in the i -th feature SHAP knowledge sub-bases. Each feature SHAP knowledge sub-base contains: (1) feature values discretized with fixed step sizes, and (2) their corresponding averaged SHAP values within defined ranges.

This grouping mechanism enables effective alignment between individual feature instances and their subgroup SHAP distributions, facilitating coherent information utilization. However, it is still difficult for LLMs to utilize SHAP values.

2.2.4 Probabilistic Interpretation of SHAP Values

To address the interpretability of SHAP values, we chose to transform them into a structured format optimized for LLMs, rather than relying on resource-intensive domain knowledge integration. This approach minimizes token consumption while enabling the LLM to generate contextually relevant explanations from preprocessed feature importance signals.

We implement a probabilistic transformation framework, combining Sigmoid Normalization:

$$\sigma(\varphi_i) = \frac{1}{1 + e^{-\varphi_i}}$$

where φ_i represents the original SHAP value, converting feature contributions into normalized probabilities (0-1 range)

For a model f and instance x , SHAP value φ_i satisfy:

$$f(x) = \varphi_0 + \sum_{i=1}^M \varphi_i(x)$$

where $\varphi_0 = E[f(x)]$ is the base value.

For specific feature impact analysis, we compute differential contributions through Contrastive Attribution Calculation using Sigmoid (CACS):

Let $z = \varphi_0$ The probability contribution p_j of j interval mean SHAP value is defined as:

$$p_i = \sigma(z + \varphi_j) - \sigma(z)$$

Where σ is the sigmoid function.

By computing probability contributions for all interval mean SHAP values, we establish an **Average Contribution Probability Base** for LLMs:

CACS(SHAP Knowledge Base) = Average Contribution Probability Base
Specifically:

$$\text{Average Contribution Probability Base} = \begin{bmatrix} b_1 \\ b_2 \\ \vdots \\ b_{15} \end{bmatrix} = \begin{bmatrix} p_{1,1} & p_{1,2} & \cdots & p_{1,k_1} \\ p_{2,1} & p_{2,2} & \cdots & p_{2,k_2} \\ \vdots & \vdots & \ddots & \vdots \\ p_{15,1} & p_{15,2} & \cdots & p_{15,k_{15}} \end{bmatrix}$$

Where b_i is the i -th feature sub-bases in Average Contribution Probability Base, p is the contribution probability and k_i is the length of contribution probability values in the i -th feature sub-bases in Average Contribution Probability Base.

This framework enables systematic characterization of feature impacts for new incoming feature values, providing a probabilistic foundation for interpretable model analysis.

2.3 Module (B) Cross-Model Knowledge Distillation

After the processing described in previous sections, we successfully translated the XGBoost model's decision logic into a LLMs interpretable format and constructed an Average Contribution Probability Base (ACPB) tailored for LLMs. However, the ACPB alone encapsulates only the XGBoost-derived knowledge. To fully integrate the complementary strengths of XGBoost's predictive accuracy and LLMs' natural language reasoning capabilities, we introduce a Cross-Model Knowledge Distillation (CMKD) framework (Figure 3), which enables bidirectional knowledge transfer and consensus building between the two paradigms.

This framework not only preserves the structural insights from XGBoost but also leverages LLMs to generate human-readable explanations, bridging the gap between predictive performance and clinical interpretability.

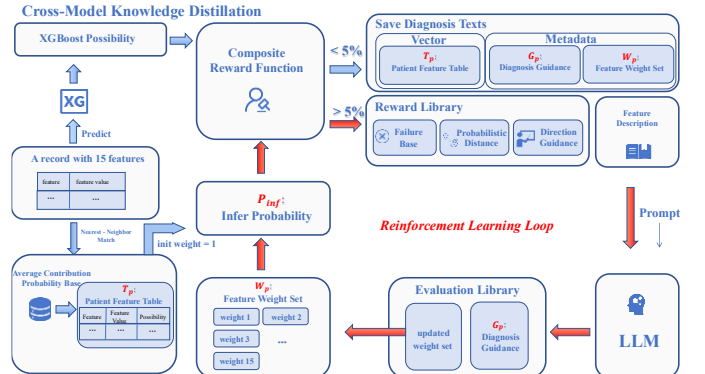


Figure 3. The Reinforcement Learning Loop for knowledge distillation and diagnostic text generation. This diagram details Module (B) of the framework. For a given patient case, an initial Infer Probability is calculated using the Average Contribution Probability Base and an initial weight set. This is compared against the XGBoost Probability via a Composite Reward Function. If the difference is greater than 5%, the Reinforcement Learning Loop is activated. The Reward Library provides feedback to the LLM, which then generates an Evaluation Library containing updated feature weights and diagnostic guidance. This loop iterates until the Infer Probability aligns with the XGBoost Probability, at which point the refined diagnostic text and metadata are saved.

As illustrated in the flowchart, the proposed framework for generating high-quality medical diagnostic texts initiates with extracting structured clinical features from patient records. Each record contains 15 clinical features that are matched with Average Contribution Probability Base to construct a Patient Feature Table. The initial probability inference employs a uniform feature weight set (all weights initialized to 1) during the first computation cycle. When evaluated by the composite reward function, if the discrepancy between Infer Probabilities and XGBoost Probabilities falls below a predefined threshold, the system preserves outputs containing metadata and retrieval vectors.

Should the discrepancy exceed this threshold, a reinforcement learning loop activates: Composite Reward Library generates a Reward Library, comprising Failure Base, Probability Distance, and Direction Guidance modules, that drive LLMs to synthesize an Evaluation Library with feature descriptions. This process yields updated feature weights and diagnostic guidance, which subsequently inform the next probability inference iteration, thus enhancing the LLM's diagnostic text generation performance through iterative refinement.

Pseudocode is as follows:

Algorithm 1 Cross - Model Knowledge Distillation Framework

```

Require: A record with 15 features (f_1, f_2, ..., f_15), weight set (w_1, w_2, ..., w_15)
        Average Contribution Probability Base (ACPB)
        Pre-trained LLM
        Reward threshold ε

Ensure: Saved high-quality diagnostic texts

1: for each patient record R in the dataset do
2:   (ConPro_1, ConPro_2, ..., ConPro_15) ← R
Nearest Match with ACPB 3: Patient Feature Table
T_p ← (ConPro_1, ConPro_2, ..., ConPro_15) /UR
4:   Initial Weight Set ← set all weights to 1
5:   Initial P_inf ← ProbCalculation(T_p, initial weight set)
6:   diff ← Calculate diff ← Composite Reward
Function(initial P_inf, P_true)
7:   if diff > ε then
8:     Diagnosis Guidance G_p ← LLM ←
Prompt(T_p, Feature Description)
9:     Save(Vector: T_p, Metadata: G_p, w_p)
10:   else
11:     while diff ≥ ε do
12:       Reward Library ← Composite Reward
Function(initial P_inf, P_true)
13:       Evaluation Library ← LLM ←
Prompt(Reward Library, Feature Description)
14:       Updated Weights, Diagnosis Guidance
G_p ← Evaluation Library
15:       Weight Set W_p ← Updated Weights
16:       P_inf ← ProbCalculation(T_p, Weight
Set)
17:       diff ← Calculate diff(P_inf, P_true)
18:       if diff ≤ ε then
19:         Save(Vector: T_p, Metadata: G_p,
W_p)
20:       Break
21:     end if
22:   end while
23: end if
24: end for

```

Comprehensive technical specifications for core modules (feature extraction, probability inference, composite reward evaluation, and reinforcement learning mechanisms) are systematically elaborated in subsequent sections.

2.3.1 State Representation and cold start strategy

The diagnostic state is defined:

$$s = (T_p, W_p, P_{inf}, G_p)$$

where T_p : Patient Feature Table containing 15-features clinical indicators.

W_p : Feature weight indicates the feature probability impact.

P_{inf} : Infer probability that calculated through weights and contribution probabilities.

G_p : Guidance that forming from LLMs' feature analysis.

This state space design achieves: 1) Complete encoding of patient features and feature contributions. 2)Dynamic weight adjustment foundation. 3)Interpretable probability generation mechanism.

In the initial probability inference, we only inject the prior XGBoost knowledge by setting *init weights* = 1 as the cold - start strategy. By doing so, we assume that all initial diagnostic outcomes are exclusively derived from prior knowledge associated with the XGBoost. This approach provides a fair starting point for the LLMs, allowing it to consider all features without bias. It also simplifies the initial calculation of the infer probability, as the contribution of each feature is initially treated equally.

The probability calculation formula as follows:

$$\text{Infer Probability} = \text{Base Probability} + \sum_{i=1}^{15} (\text{Contribution Probability}_i \times \text{Weight}_i)$$

where *Base Probability* equals 0.5.

If the infer probability is sufficiently close to XGBoost Probability, it suggests that the initial weights do not necessitate adjustment. In such a scenario, the initial weight set, Patient Feature Table, and the prompt are jointly fed into the Large Language Models (LLMs) to generate Diagnosis Guidance. Subsequently, these generated texts are stored in Qdrant.

2.3.2 Composite Reward Function Design

We propose a dynamic reward mechanism based on probabilistic deviation, aiming to provide large language models (LLMs) with explicit optimization direction and intensity. The mechanism maintains a **Reward Library** to achieves fine-grained evaluation through dual constraints of **Probabilistic Distance Quantification Mechanism** and **Optimization Direction Guidance Mechanism**, with experience replay by **Failure Case Base Maintenance**.

If we successfully gain the proper infer possibility, the mechanism can save the diagnosis texts by Qdrant.

Probabilistic Distance Quantification Mechanism

The proposed quantification mechanism is designed to ensure precise optimization of LLMs by dynamically balancing directional correctness through probabilistic deviation quantification and decision boundary alignment while maintaining adaptive penalization gradients and training stability, with its core formula defined as:

$$Score = \begin{cases} f(\cdot), & \text{diff} > 0.05 \text{ and } S(\cdot) > 0 \\ 10, & \text{diff} \leq 0.05 \text{ and } S(\cdot) > 0 \\ 0, & S(\cdot) < 0 \end{cases}$$

where

$$diff = \frac{|True\ Probability - Infer\ Probability|}{True\ Probability} \quad \text{quantifies the}$$

relative deviation between predicted and true probabilities;

$$S(\cdot) = (True\ Probability - 0.5) \times (Infer\ Probability)$$

determines whether the prediction aligns with the true decision boundary (0.5);

$$f(\cdot) = \frac{True\ Probability}{|True\ Probability - Infer\ Probability|} \quad \text{inverse-proportional}\newline \text{penalties on high-deviation predictions to enhance error}\newline \text{sensitivity.}$$

Optimization Direction Guidance Mechanism for LLMs

To enhance the interpretability and actionability of Composite Reward Function, we translate mathematical reward signals into explicit natural language instructions. This mechanism bridges probabilistic deviations with human-readable feedback, enabling LLMs to dynamically adjust their reasoning paths toward the correct answer.

We trust the natural language instruction maps the reward function outputs ($diff, S(\cdot)$) to structured textual guidance using conditional logic:

$$Guidance = \begin{cases} \text{Your inferred probability is } \begin{cases} \text{significantly higher than actual levels} & \text{diff} > 0.05 \text{ and } S(\cdot) > 0 \\ \text{significantly lower than actual levels} & \text{diff} < 0.05 \text{ and } S(\cdot) > 0 \end{cases} \\ \text{Prediction direction correct with acceptable deviation, } \text{diff} < 0.05 \text{ and } S(\cdot) > 0 \\ \text{Warning: Prediction contradicts factual direction. Re-examine decision basis, } S(\cdot) < 0 \end{cases}$$

Building upon the dynamic reward mechanisms that bridge mathematical precision and semantic interpretability, these instructions contextualize them within decision boundaries and point out the optimization direction, enabling LLMs to iteratively refine their reasoning trajectories.

Failure Case Base Maintenance

To improve probability estimation accuracy, we maintain a dynamic Failure Case Base that stores instances where the model's predicted probability significantly deviates from the true probability ($diff > 0.05$). The base operates under the following update rules:

When encountering a failure case and the base contains fewer than three instances, the new case is added directly. At maximum capacity (three cases), the oldest failure case is removed (FIFO replacement) before adding the new one. The stored cases are used to guide the model's probability calibration, helping it converge toward true probability estimates [18].

This selective retention mechanism ensures the model continuously learns from recent, representative prediction errors while maintaining a manageable case base size. The 0.05 threshold and three-case limit were empirically determined to balance calibration effectiveness with computational efficiency.

Saving diagnosis texts using Qdrant

If the deviation between the infer probability calculated by a specific formula from the feature weights generated by DeepSeek - R1 - 8B and the XGBoost probability is within 5% ($diff > 0.05$), and based on this infer probability, it is possible to accurately determine whether there is sarcopenia or not, then this diagnostic text will be saved in a special structure. The special structure considers Patient Feature Table as the retrieve

vector and both weight set and diagnosis guidance as the metadata.

Following the generation of diagnostic texts using 324 training samples, we constructed a **Diagnosis Knowledge Base (DKP)**. This knowledge base enables retrieval of historical diagnostic records via the Patient Feature Table, thereby facilitating the large language model (LLM) to leverage prior XGBoost and LLMs knowledge for improving prediction accuracy.

2.3.3 LLM Policy Optimization

In the data preprocessing phase, the application of the Hierarchical Adaptive Group Averaging (HAGA) method yielded a group-average SHAP representation, albeit at the cost of attenuating patient-specific granularity. To mitigate this limitation, we introduce a dynamic weight adjustment mechanism that simultaneously recovers individualized diagnostic signals and infuses domain knowledge derived from the LLM. A policy network is constructed based on DeepSeek-R1-8B, with a decision-making process as follows:

Feature Analysis:

Based on insights from **Reward Library** and basic clinical knowledge derived from **Feature Description**, large language models (LLMs) dynamically refine the assessment of each feature's impact, thereby constructing a novel framework for feature analysis. In this process, LLMs integrate contribution probability from XGBoost to quantify the statistical significance of features, while simultaneously applying multi-features reasoning to assign adaptive weights. For instance, LLMs tend to prioritize rare but pathognomonic symptoms over more common yet fewer indicative features. Ultimately, the Feature Analysis yields Diagnosis Guidance, offering knowledge-informed support for clinical decision-making.

Weight Adjustment:

Leveraging the results of Feature Analysis, LLMs derive context-aware feature weights to generate a new, optimized set of weights [17]. This updated Weight Set combines the machine learning insights from XGBoost with the clinical reasoning capabilities of the LLM, achieving a more holistic and adaptive representation of feature importance.

After LLM Policy Optimization, we gain the Evaluation Library which consists of both the Diagnosis Guidance and the updated Weight Set. The Diagnosis Guidance provides interpretability and traceability by explaining the reasoning behind feature contributions, while the updated Weight Set enables recalculation of inference probabilities. Together, they support a context-sensitive and clinically relevant diagnostic process.

This architecture effectively transforms the group-average representation into patient-specific inferences while maintaining diagnostic validity.

2.4 Module (C) Prediction & Context-Aware Reasoning

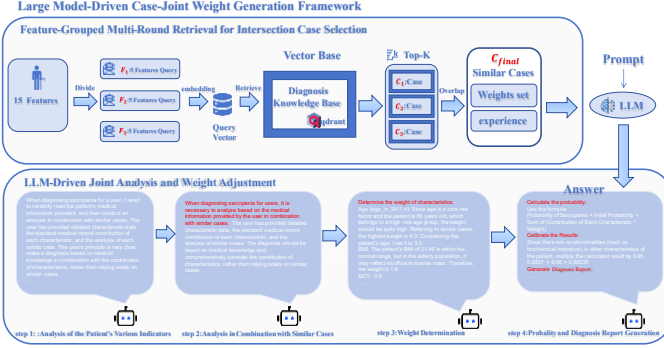


Figure 4. The architecture for Prediction & Context-Aware Reasoning. This diagram illustrates Module (C). For a new patient with 15 features, the Feature-Grouped Multi-Round Retrieval (FGMR) method queries the Diagnosis Knowledge Base to find a set of semantically similar cases (C_{final}). The features of the new patient, along with the retrieved similar cases (including their feature weights and diagnostic text), are fed as a comprehensive prompt into the LLM. The LLM then performs a joint analysis to generate a final, context-aware prediction and a detailed report.

This method presents an integrated diagnostic framework combining Feature-Grouped Multi-Round Retrieval for Intersection Case Selection and LLM-Driven Joint Analysis and Weight Adjustment, shown in Figure 4. First, 15 clinical features are divided into three subsets for parallel case retrieval, with intersecting results ensuring cross-feature consistency. The system then employs LLMs to: (1) generate initial diagnoses, (2) refine them through similar case comparisons, and (3) produce adaptive feature weights. (4) Finally, calculate the sarcopenia probability and generate the diagnosis report. This approach enables precise, interpretable diagnoses by bridging statistical patterns with clinical reasoning, shown in figure 4.

Pseudocode is as follows:

Algorithm 2 Prediction & Context-Aware Reasoning Framework

```

1: Input: Feature vector X = [x_1, x_2, ..., x_15]
2: Output: Diagnosis Prediction via LLM
3: Divide X into 3 groups: F_1, F_2, F_3, where F_i ∈ R^5
4: for i = 1 to 3 do
5:   Encode feature group F_i into query vector q_i = Embed(F_i)
6:   Retrieve top-k similar cases: C_i = TopK(Retrieve(q_i))
7: end for
8: Similar Cases ← Compute intersection of
   retrieved cases: C_final = ∩^3_{i=1} C_i
9: Weight Set W_p, Diagnosis Guidance G_p ← Similar
   Cases
10: Diagnosis Prediction ← LLMs ← Prompt(W_p, G_p)

```

2.4.1 Feature-Grouped Multi-Round Retrieval for Intersection Case Selection

We propose a method named Feature-Grouped Multi-Round Retrieval for Intersection Case Selection (FGMR) retrieval, to identify cases consistently detected across three feature subsets. Fifteen features are evenly divided into three groups (F_1, F_2, F_3 , 5 features each) [19]. For each group will be sent to Qdrant as feature query to retrieve cases C_k , using BGE-Embedding-1024 and BEG-Reranker (Top-k, k=8) with a cosine similarity

threshold 0.7. The final selection is the intersection of the three retrieval results:

$$C_{final} = C_1 \cap C_2 \cap C_3$$

ensuring cases are detected by all feature queries.

2.4.2 LLM-Driven Sarcopenia Prediction and Report Generation

After applying the FGMR retrieval method and obtaining similar cases that embody the correct state, large language models (LLMs) initially conduct an independent assessment of the patient's condition to formulate an initial diagnostic hypothesis. This hypothesis is then refined by integrating analogous cases, a process that promotes the iterative improvement of the analytical framework. From the refined conclusion, LLMs generate personalized weight parameters, which form the basis for calculating probabilistic outputs, and calculate the final sarcopenia probability.

Subsequently, by quantifying the contribution probabilities of feature interactions, the model determines the relative influences of different features. Simultaneously, the weights allow for the identification of the specific ways in which these features affect the diagnostic process. Through this dual - learning mechanism — using probabilistic contributions to model feature importance and weight assignments to describe feature interactions — LLMs systematically produce a structured diagnostic report that combines empirical evidence, analytical reasoning, and case - based correlations.

Pseudocode is as follows:

Algorithm 3 LLM-Driven Sarcopenia Prediction and Report Generation.

```

1: Input: Patient data D_p, FGMR retrieval method
R
2: Output: Final probability P_sarc and diagnostic
report R_diag
3: C ← R(D_p)                                ▷ Retrieve similar
   cases using FGMR
4: H_0 ← LLM_Assess(D_p)                      ▷ Initial hypothesis
   by LLM
5: H ← Refine(H_0, C)                          ▷ Refine hypothesis
   using retrieved cases
6: W ← GenerateWeights(H, C)                  ▷ Generate
   personalized weights
7: P_sarc ← ComputeProbability(D_p, W)        ▷ Calculate
   sarcopenia probability
8: F_c ← QuantifyContributions(D_p, W)        ▷ Feature
   contribution probabilities
9: F_c ← ModelFeatureImportance(F_c, W)       ▷ Evaluate
   feature influence and interactions
10: R_diag ← GenerateReport(H, F_c, C)        ▷ Generate
   structured diagnostic report
11: return P_sarc, R_diag

```

RESULT

3.1 Comparison of Prediction Results of Sarcopenia

Due to the extremely complex characteristics of sarcopenia and the existence of many data types, we use XGBoost as the teacher model of the large model. XGBoost supports multiple data types and allows the combination of tree models and linear models (referred to as GBDT+linear) within one model, which enhances the expressive ability of the model, further improves the prediction performance, and can flexibly handle complex nonlinear and linear problems.

In the prediction of sarcopenia using LLMs, we adopt a voting mechanism and determine the final result through a majority vote, which improves the reliability and stability of the prediction results. Specifically, for each case to be predicted, the LLM is used to conduct three independent predictions. If a certain prediction result appears twice or more, it will be determined as the final prediction conclusion. The outcomes showcased consistent improvements, as outlined in Table 1.

Table 1. Performance comparison of different models for sarcopenia prediction. The table evaluates various models based on precision, recall, F1-score, and accuracy for both normal and abnormal classes. The proposed model, Deepseek-R1-8B with reinforcement training, achieves the highest accuracy (0.96) and demonstrates superior performance across most metrics compared to the baseline XGBoost, Random Forest, Decision Tree, and the LLM without specialized training.

Model	Result Evaluation(normal/abnormal)(%)				
	Method	Precision	Recall	F1score	Accuracy
XGBoost	/	0.82/0.9	0.64/0.79	0.72/0.68	0.70
Random Forest	/	0.84/0.68	0.75/0.79	0.79/0.73	0.77
Decision Tree	/	0.75/0.62	0.75/0.62	0.75/0.62	0.7
Deepseek-R1-8B	/	0.55/0.34	0.47/0.47	0.51/0.38	0.45
Deepseek-R1-8B	SHAP Knowledge XGBoost	0.85/0.61	0.64/0.83	0.73/0.70	0.72
Deepseek-R1-8B	SHAP Knowledge Reinforcement Train XGBoost	0.96/0.72	0.75/0.96	0.84/0.82	0.83

3.2 Contribution Probability using Sigmoid Analysis

To verify the absence of significant statistical bias in the proposed contribution probability calculation method, this study conducted a systematic comparative analysis between the predicted probabilities generated by the XGBoost model and the inferred probabilities of corresponding samples in the training dataset. The inferred probabilities were defined as the sum of the contribution probability matching the Average Contribution Probability Base and the base probability (0.5). Specifically, we calculated the absolute differences between these two sets of probabilities and performed statistical analysis on the resulting values. The analytical results are presented as follows:

Table 2. Statistical analysis of the bias between XGBoost probabilities and inferred probabilities from the proposed CACS method. The table presents the mean, standard deviation (Std), median, minimum (Min), and maximum (Max) of the absolute differences between the two probability sets on the training data. The low mean absolute error of 0.01729 demonstrates a high degree of consistency and validates the effectiveness of the contribution probability calculation method.

Bias Analysis	Mean	Std	Median	Min Bias	Max Bias
	0.01729	0.01222	0.01414	0.00014	0.0632

Statistical analysis revealed a mean absolute error of 1.729% between the predicted and contribution probabilities,

demonstrating high consistency. This low error margin supports the validity of our method for estimating sarcopenia probability in clinical applications.

3.3 Cross-Architectural Knowledge Distillation Analysis

While prior studies have demonstrated the efficacy of cross-architectural knowledge distillation from XGBoost to large language models (LLMs), a systematic evaluation of their predictive congruence remains critical to validate that the enhanced predictive capabilities of LLMs are directly attributable to the distilled knowledge from XGBoost, rather than inherent architectural advantages or task-specific biases. By conducting a quantitative and qualitative assessment of class-wise decision boundaries and error distributions (e.g., via confusion matrix decomposition and feature attribution analysis), we further elucidate the mechanistic alignment between the distilled LLM and its XGBoost teacher, thereby establishing a robust foundation for interpreting the knowledge transfer efficacy in heterogeneous model frameworks.

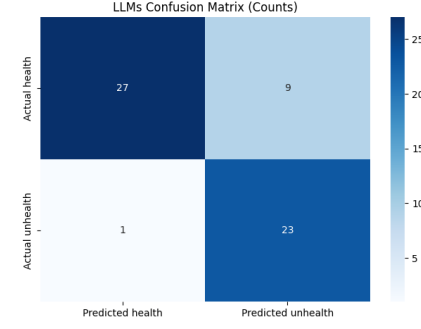


Figure 5. LLM Confusion Matrix: This matrix displays the performance of the LLM (Deepseek-R1-8B with reinforcement training). It shows that out of 33 "health" samples, 29 were correctly identified as "health" (true negatives), while 4 were misclassified as "unhealth" (false positives). For the 24 "unhealth" samples, 23 were correctly identified as "unhealth" (true positives), and only 1 was misclassified as "health" (false negative).

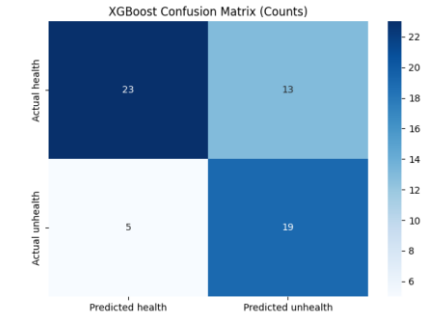


Figure 6. XGBoost Confusion Matrix: This matrix displays the performance of the baseline XGBoost model. It shows that out of 37 "health" samples, 27 were correctly identified as "health" (true negatives), while 10 were misclassified as "unhealth" (false positives). For the 29 "unhealth" samples, 24 were correctly identified as "unhealth" (true positives), and 5 were misclassified as "health" (false negatives).

As illustrated in Figure 5 (LLMs) and Figure 6 (XGBoost), the confusion matrices reveal notable similarities in **error distribution trends and class-specific decision biases** between the two architecturally distinct models (neural

networks vs. tree-based models), despite differences in absolute performance:

Both models exhibit a higher proportion of false positives (FP) compared to false negatives (FN) for the majority class. Specifically, LLMs misclassify 9/36 (25%) of "health" samples as "unhealth" (FP), while XGBoost misclassifies 13/36 (36.1%). This shared conservative bias toward labeling "health" samples as "unhealth" suggests alignment in prioritizing avoidance of critical FN errors, potentially influenced by imbalanced training data or task-specific cost sensitivity. Primary errors for both models are concentrated in FP misclassifications ("health" to "unhealth"), with LLMs and XGBoost showing proportional FP magnitudes (9 vs. 13). This proportional consistency in error distribution implies that, despite architectural divergence, LLMs distilled most knowledge, correct or not, from XGBoost.

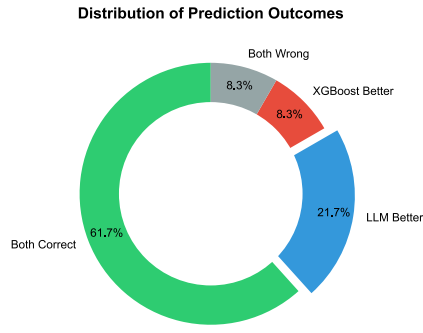


Figure 7. Concordance analysis of prediction outcomes between the LLM and XGBoost. The chart shows that both models were correct for 61.7% of cases and both were wrong for 8.3%. In 30% of cases where they disagreed, the LLM was correct more often (21.7%) than the XGBoost model (8.3%). This indicates that the LLM not only distilled knowledge but also improved upon the teacher model's predictions.

The consistency analysis between LLMs and XGBoost reveals several key insights into their predictive behaviors and knowledge transfer dynamics. As shown in Figure X, the models exhibit a 70% agreement rate (61.7% Both Correct + 8.3% Both Wrong), with 30% of predictions being discordant (21.7% LLM Better + 8.3% XGBoost Better). This pattern implies that LLMs have effectively distilled not only correct predictions but also systematic errors from the XGBoost model, demonstrating the depth of the knowledge transfer process.

Further examination of correct prediction sources provides granular understanding of this relationship. The models jointly achieve correct predictions for 61.7% of samples, confirming strong baseline alignment. More revealing is the 21.7% of cases where only LLMs are correct, much higher than 8.3% of XGBoost correction only, - these predominantly involve longer contexts composed of enough similar cases, as well as the LLM reasoning capabilities.

More specific comparison shown in Figure 8:

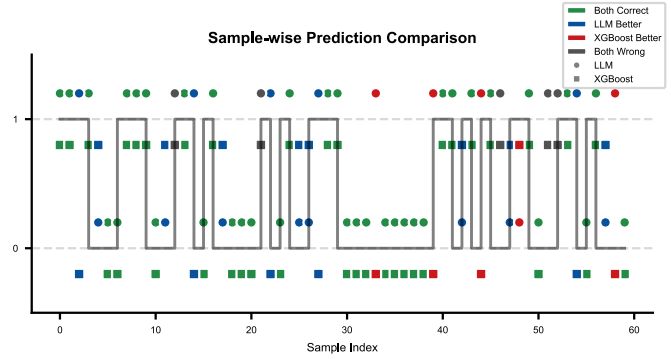


Figure 8. Sample-wise prediction comparison between LLM and XGBoost. This plot visualizes the prediction outcome for each sample in the test set. Green squares indicate instances where both models were correct. Blue circles represent cases where only the LLM was correct, while red squares show cases where only XGBoost was correct. Black 'x' marks denote instances where both models failed. The ground truth is represented by the solid black line (1 for unhealth, 0 for health).

DISCUSSION

This study introduces the LLM-Adapted Interpretation (LAI-ML) framework, a hybrid architecture that integrates the statistical precision of gradient-boosted models with the contextual reasoning of large language models. Designed to enhance both predictive accuracy and interpretability, LAI-ML demonstrates that such synergy is feasible and impactful in clinical decision support.

The framework achieved 83% accuracy in predicting sarcopenia risk, outperforming both the standalone XGBoost model (70%) and an untrained LLM (45%) [1]. More importantly, LAI-ML corrected 21.7% of XGBoost's misclassifications, while the reverse occurred in only 8.3% of cases, suggesting the LLM extends beyond imitation and adds independent inferential capacity. This capability arises from the architecture's dual-stream design, where the LLM fuses knowledge distilled from XGBoost with context-rich patient analogs retrieved via Feature-Grouped Multi-Round Retrieval (FGMR). Such a structure allows LAI-ML to uncover complex, nonlinear relationships overlooked by tree-based methods, aligning with the principles of augmented intelligence [19].

Beyond performance, the framework contributes a model-agnostic pipeline for explainability. The proposed Half-step Aligned Group Averaging (HAGA) and Contrastive Attribution via Sigmoid (CACS) methods translate SHAP attributions into stable, interpretable formats. HAGA reduces volatility by discretizing feature values and aggregating SHAP scores, while CACS converts them into probabilistic contributions using sigmoid differentials. The resulting transformation preserves fidelity, with a mean absolute error of just 1.729% when compared to original XGBoost outputs. This pipeline facilitates alignment between quantitative attribution and LLM-based reasoning, advancing the field toward deeply integrated XAI [20].

Clinically, LAI-ML replaces opaque predictions with reasoned, defensible diagnostic narratives. Instead of returning raw risk scores, the framework provides structured reports grounded in feature attributions and precedent cases. When diverging from

the teacher model, LAI-ML generates traceable justifications (e.g., reweighting features based on case-based evidence), offering clinicians actionable insights. This transition from explainable to *defensible and actionable AI* is essential for adoption in high-stakes settings such as medicine, where transparency and trust are critical [21].

Nevertheless, several limitations must be addressed. The model was trained and evaluated on a single dataset (CHARLS), limiting generalizability. Validation on other cohorts, such as NHANES or ELSA, is necessary to ensure fairness and robustness across populations. Additionally, while effective with the XGBoost-LLM pairing, the framework's adaptability across other model combinations remains unexplored. The discretization in HAGA, while stabilizing, may obscure patient-level nuance; future work should explore adaptive or learned transformations. Lastly, the computational cost of reinforcement training and multi-round retrieval could hinder real-time deployment, necessitating optimization strategies such as quantization and efficient indexing.

CONCLUSION

The LAI-ML framework represents a significant advancement in interpretable and collaborative artificial intelligence. By integrating a statistical model with a generative reasoning engine, it delivers accurate, context-aware, and explainable diagnostic outputs. Unlike conventional distillation approaches, LAI-ML enables the LLM to refine and, in many cases, surpass the predictions of its teacher model through a combination of distilled knowledge and case-based reasoning.

Through its generalizable semantic attribution pipeline and evidence-grounded reporting structure, LAI-ML addresses core challenges in clinical AI: transparency, accountability, and usability. This work offers a scalable blueprint for deploying AI systems as reliable partners in high-stakes domains, ultimately empowering clinicians with interpretable and defensible decision support.

CONFLICT OF INTEREST

The authors report no conflict of interest. We did not participate in recruiting the participants, as this article is based on publicly available data from the NHANES in the US. Since written informed consent was obtained from all participants in NHANES, this study was exempt from ethics review approval.

FUNDING

This study was funded by the XXX.

DATA AVAILABILITY

Data described in the manuscript, code book, and analytic code will be made publicly and freely available without restriction at <https://www.cdc.gov/nchs/nhanes/index.htm>. The analytic code will be made available upon request pending application and approval from the corresponding author.

REFERENCES

- [1] Cruz-Jentoft AJ, Baeyens JP, Bauer JM, Boirie Y, Cederholm T, Landi F, Martin FC, Michel JP, Rolland Y, Schneider SM, et al. Sarcopenia: European consensus on definition and diagnosis: report of the European working group on sarcopenia in older people. *AGE AGEING*. 2010;39(4):412–23.
- [2] Tianqi Chen and Carlos Guestrin. 2016. XGBoost: A Scalable Tree Boosting System. In Proceedings of the 22nd ACM SIGKDD International Conference on Knowledge Discovery and Data Mining (KDD '16). Association for Computing Machinery, New York, NY, USA, 785–794.
- [3] Chen, X., & Li, L. (2025). Prediction of sarcopenia at different time intervals: an interpretable machine learning analysis of modifiable factors. *BMC geriatrics*, 25(1), 133.
- [4] Thirunavukarasu, A.J., Ting, D.S.J., Elangovan, K. et al. Large language models in medicine. *Nat Med* **29**, 1930–1940 (2023). <https://doi.org/10.1038/s41591-023-02448-8>
- [5] Yue Zhang, Yafu Li, Leyang Cui, Deng Cai, Lemao Liu, Tingchen Fu, Xinting Huang, Enbo Zhao, Yu Zhang, Yulong Chen, Longyue Wang, Ahn Tuan Luu, Wei Bi, Freda Shi, Shuming Shi; *Siren's Song in the AI Ocean: A Survey on Hallucination in Large Language Models*. *Computational Linguistics* 2025
- [6] Schaaf, J., Sedlmayr, M., Sedlmayr, B., Prokosch, H. U., & Storf, H. (2021). Evaluation of a clinical decision support system for rare diseases: a qualitative study. *BMC medical informatics and decision making*, 21(1), 65.
- [7] Winter, P. D., & Carusi, A. (2023). (De) troubling transparency: artificial intelligence (AI) for clinical applications. *Medical Humanities*, 49(1), 17-26.
- [8] Nazary, F., Deldjoo, Y., Di Noia, T., & Di Sciascio, E. (2024). Xai4llm. let machine learning models and llms collaborate for enhanced in-context learning in healthcare. *arXiv preprint arXiv:2405.06270*.
- [9] Stangel, P., Bani-Harouni, D., Pellegrini, C., Özsoy, E., Zaripova, K., Keicher, M., & Navab, N. (2025). Rewarding doubt: A reinforcement learning approach to confidence calibration of large language models. *arXiv e-prints*, arXiv-2503.
- [10] Kriz, A., Janes, E. L., Shen, X., & Arbel, T. (2025). Prompt4Trust: A Reinforcement Learning Prompt Augmentation Framework for Clinically-Aligned Confidence Calibration in Multimodal Large Language Models. *arXiv preprint arXiv:2507.09279*.
- [11] Zou X, He W, Huang Y, Ouyang Y, Zhang Z, Wu Y, Wu Y, Feng L, Wu S, Yang M, Chen X, Zheng Y, Jiang R, Chen TAI-Driven Diagnostic Assistance in Medical Inquiry:

Reinforcement Learning Algorithm Development and
Validation
J Med Internet Res 2024;26:e54616

[12] Fansi Tchango, A., Goel, R., Martel, J., Wen, Z., Marceau Caron, G., & Ghosn, J. (2022). Towards trustworthy automatic diagnosis systems by emulating doctors' reasoning with deep reinforcement learning. *Advances in Neural Information Processing Systems*, 35, 24502-24515.

[13] Liu, J., Wang, W., Ma, Z., Huang, G., SU, Y., Chang, K. J., ... & Lyu, M. (2024). Medchain: Bridging the gap between llm agents and clinical practice through interactive sequential benchmarking. *arXiv preprint arXiv:2412.01605*.

[14] Zhao, Y., Hu, Y., Smith, J. P., Strauss, J., & Yang, G. (2014). Cohort profile: the China health and retirement longitudinal study (CHARLS). *International journal of epidemiology*, 43(1), 61-68.

[15] Nohara, Y., Matsumoto, K., Soejima, H., & Nakashima, N. (2022). Explanation of machine learning models using shapley additive explanation and application for real data in hospital. *Computer Methods and Programs in Biomedicine*, 214, 106584.

[16] Jullum, M., Redelmeier, A., & Aas, K. (2021). groupShapley: Efficient prediction explanation with Shapley values for feature groups. *arXiv preprint arXiv:2106.12228*.

[17] Andrychowicz, M., Wolski, F., Ray, A., Schneider, J., Fong, R., Welinder, P., ... & Zaremba, W. (2017). Hindsight experience replay. *Advances in neural information processing systems*, 30.

[18] Chen, Y., Gao, J., & Wu, J. (2024). Dynamic feature selection in medical predictive monitoring by reinforcement learning. *arXiv preprint arXiv:2405.19729*.

[19] Deep medicine, artificial intelligence, and the practising clinician. Matuchansky, Claude *The Lancet*, Volume 394, Issue 10200, 736

[20] S. Lundberg and S.-I. Lee, "A Unified Approach to Interpreting Model Predictions," in *Proc. NeurIPS*, 2017, pp. 4765–4774.

[21] E. Tjoa and C. Guan, "A Survey on Explainable Artificial Intelligence (XAI): Toward Medical XAI," in *IEEE Transactions on Neural Networks and Learning Systems*, vol. 32, no. 11, pp. 4793-4813, Nov. 2021.